Ballistic Range

Sen Liu

Ballistic range is a kind of test facility, in which the test models or projectiles are launched at desired velocity, the aerodynamic properties of the flying models are measured during its flight, or shock and damage of the targets are measured upon the projectile impact.

Originally developed for studying the flight and/or lethality of bullets or artillery shells in 18th century, the ballistic range was adapted as a powerful facility for the study of high speed flight vehicles since World War Two, with the advent of the Aerodynamic Range at the US Army Aberdeen Proving Ground in 1943. The range is noted as "the world's first large-scale, fully-instrumented ballistic range reproducing data on the aerodynamic characteristics of missiles in free flight" [1].

With the invention of two-stage light gas gun by Crozier in 1946 and Hume in 1950s [2], ballistic range was widely used in the fields of hypervelocity aerothermodynamics and hypervelocity impact effects since the 1950s, as the results of the developments of hypervelocity reentry vehicles, protection of structures/shields against space debris, and kinetic energy weapons.

1 Introduction

Ballistic range has a long history in the development of ordnance, such as bullets, artillery shells, rifles, cannons, and warheads. In 1742, a primitive ballistic range was developed by Benjamin Robins to measure the velocity of a projectile fired from a cannon. The measurement device used by him is a ballistic pendulum.

By the end of 19th century, cannon shell design was evolved from spherical to streamlined configuration to reduce aerodynamic drag. To sustain flight stability, the streamlined shell must spin very fast. At this time, the role of ballistic range was

S. Liu (✉)
Hypervelocity Aerodynamics Institute (HAI), China Aerodynamics Research and Development Center (CARDC), Mianyang 621000, Sichuan Province, People's Republic of China
e-mail: liusen@cardc.in

© Springer International Publishing Switzerland 2016

F. Seiler and O. Igra (eds.), *Hypervelocity Launchers*,
Shock Wave Science and Technology Reference Library 10,
DOI 10.1007/978-3-319-26018-1_2

not only to measure projectile velocity, but also measure the flight attitude of the projectile. To meet these requirements, solenoid coils and ballistic cardboard techniques were developed.

During the 1930s, researchers of US Army Ballistic Research Laboratory (BRL) at Aberdeen Proving Ground started pioneering work on advanced measurement techniques of high speed projectiles. R.H. Kent, A.C. Charters and their colleagues developed techniques, such as spark shadowgraph and sequential imaging, which could record the flight of projectile with great precision. All these newly developed measurement instrumentations were adopted in the first aerodynamic ballistic range at BRL in 1943. "The range was recognized as the prototype for similar installations within the United States and abroad" [1].

Later, the knowledge obtained in the development of the aeroballistic range at BRL were applied to the construction of other famous hypervelocity ballistic ranges in the world, such as the range at NASA Ames Research Center, Range G at Arnold Engineering Development Center (AEDC), etc.

Roughly, there are two kinds of ballistic ranges. One is high speed range, which is mainly used for ordnance tests, and usually has a nearly one-atmosphere test chamber. The other is hypervelocity range, which is characterized by much higher muzzle velocity speed (e.g. faster than Mach number 5) and has a variable pressure test chamber for the simulation of high altitude in atmosphere.

With the advent of long range ballistic missile and civilian space program in the late 1940s and early 1950s, the ballistic range found new applications in the field of hypersonic aerothermodynamics and protection of spacecraft against meteoroids (and later space debris), thanked to the successful development of hypervelocity two-stage light gas gun by Crozier and Hume, and since then it became a unique and important part of ground test facilities for hypersonic aerothermodynamics and hypervelocity impact for MOD (Meteoroids and Orbital Debris) protection and kinetic weapon effects [3–10], therefore, this chapter will focus on the hypervelocity ballistic ranges.

2 Working Principle of Hypervelocity Ballistic Range

Most of hypervelocity ballistic ranges have three sub-systems, namely a launcher (usually two-stage light-gas gun) to accelerate the test model, a test section or test chamber to simulate the flight ambient conditions, such as altitude, and a measurement and control system to measure the model flight parameters and model impact and target damage parameters, as shown in Fig. 1. Shown in Fig. 2 is the 50 mm two-stage light gas gun and 200 m test chamber at Hypervelocity Aerodynamics Institute (HAI) of China Aerodynamics Research and Development Center (CARDC).

First, the test chamber is set to a desired condition, e.g. the chamber pressure; then the test model or projectile was launched at a pre-set muzzle velocity into the test chamber. If the test is to obtain aerodynamic or aero-thermodynamic properties

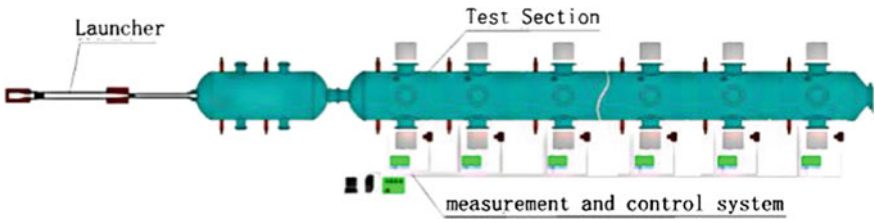

Fig. 1 Schematic of hypervelocity ballistic range

Fig. 2 Two-stage light gas gun (*upper*) and test chamber (*lower*) of 200 m free flight ballistic range at CARDC

of the model, parameters such as flight velocity, flow field structure, optical emission, and even surface pressure and heat flux would be measured during the model's flight. If the test is for hypervelocity impact effects, parameters such as projectile velocity, penetration and perforation, shock speed and temperature in target material, and debris cloud would be recorded.

The working principle of hypervelocity launcher (two-stage light gas gun), test section and measurement system will be briefly introduced.

2.1 Two-Stage Light Gas Gun

Though there are several other kinds of hypervelocity launchers, such as electro-magnetic rail gun and coil gun, the most reliable and frequently used in laboratory is the two-stage light gas gun (two-stage LGG). Compared with other launchers, the two-stage LGG has advantage in its capability of launching test models of different shapes at hypervelocity.

Since the two-stage LGG was invented by Crozier and Hume [2], many two stage LGGs have been built all over the world. Many laboratories and research institutions, such as National Aeronautics and Space Administration (NASA) Ames (USA), NASA Johnson Space Center (JSC) (USA), Arnold Engineering Development Center (AEDC) (USA), Ernst-Mach Institute EMI (Germany), French-German Research Institute of Saint-Louis (ISL) (Germany and France), HAI at CARDC, etc., have their own two-stage LGGs.

A typical two stage light gas gun consists of powder chamber/air chamber, pump tube, high pressure section, and launch tube, as shown in Fig. 3.

As its name implies, the two stage light gas gun has two stages. The first stage is the powder gun or air gun, with which a piston is accelerated in the pump tube, compressing the pre-filled light gas (e.g. hydrogen or helium). The second stage consists of the high pressure section and the launch tube. The compressed light gas (up to about 10 thousand bar) in the high pressure section accelerates the test model/projectile sabot combination.

Roughly estimated, the maximum achievable muzzle velocity is the gas escape velocity, which is attained when the gas pressure drops to zero when a complete vacuum is reached. The escape velocity is proportional to the initial gas sound speed, which is related to the molecular weight (hydrogen is lighter than helium) and temperature of the gas. The lighter the gas is, the higher is its escape velocity. Both hydrogen and helium could be used as the driving gas in the pump tube. While helium is much safer than hydrogen, the latter is considered more efficient taking into account of launch capability.

The muzzle velocity is determined by the structure of the launcher, mass of gunpowder, initial pressure of the prefilled light gas, the piston mass, the model/projectile mass, and the diaphragm pre-set rupture pressure. Interior ballistics

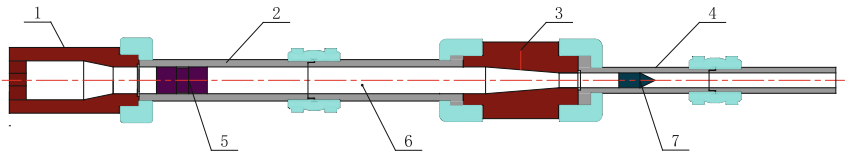

Fig. 3 Schematic of a two-stage light gas gun

analyze codes are used for finding optimal load parameters and improve the launcher design.

The piston mass is important for the optimization of a LGG. A light piston can reach high speed easily, which will form strong shock wave in the light gas, the gun turns to be a shock-heating gun, the disadvantage is obvious because of the barrel erosion. A heavy piston needs more gunpowder, and will generate a huge impact on the high pressure section.

The launch velocity is sensitive to the initial pressure of the light gas in the pump tube. Generally, the average pressure at the model base and the muzzle velocity increase with decreasing the initial light gas pressure. Though low initial pressure can yield high muzzle velocity, the erosion of gun barrel by the high temperature gas needs to be seriously considered.

Theoretically, the highest muzzle velocity that could be realized with a two-stage LGG is well above 10 km/s, and many laboratories did claim that their guns could fire a model at a velocity of 8 and even higher. However, few two-stage LGG are operated at such high velocity routinely, because of the gun barrel erosion and the model/projectile configuration. For example, the highest muzzle velocity of two-stage LGG in routine shots is about 7.5 km/s at HAI of CARDC, although the recorded highest muzzle velocity is 8.6 km/s with a 16 mm two-stage LGG.

Although most of the launch tube bore diameters of nowadays' two-stage LGGs are around ten millimeters, the biggest could be well above one hundred millimeters. The largest two stages LGG in the world is the launcher of AEDC's Range-G, with maximum bore diameter of 203 mm. Projectile velocities can reach up to 4.5 km/s for the 203 mm gun and up to 7 km/s for its inter-changeable 84 mm gun barrel [14]. The launch capability of the two-stage LGGs at AEDC and CARDC is shown in Fig. 4.

2.2 Test Chamber

As mentioned above, the role of the test chamber is to simulate flight at ambient conditions. In ballistic ranges for ordnance tests, usually there is no requirement of variable ambient pressure, so concrete-walled test chamber is a normal design, in which the projectiles fly freely and impact targets. However in those hypervelocity ballistic ranges, all the test chamber are steel or stainless steel tanks with vacuum systems, because the earth/planet atmosphere at different altitudes, or the Low Earth Orbit (LEO) condition have to be simulated in the chamber.

A test chamber usually consists of a blast tank, a test section and a diaphragm section or a fast-acting valve, and vacuum system, as shown in Fig. 5.

The blast tank, connected to the muzzle of the launcher, is used to collect the exhaust light gas which is discharged from the gun, and separate the test

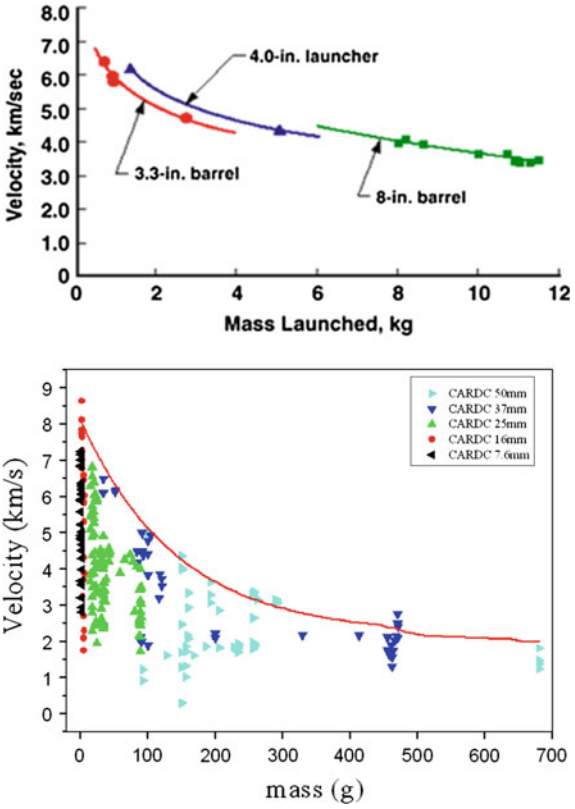

Fig. 4 Launcher capability of LGGs at AEDC [11] (*upper*) and CARDC (*lower*)

model/projectile with sabot. Between the blast tank and the test section, there is a fast-acting valve or a diaphragm, by which different pressure in blast tank and test section can be realized. The test section is one of the most important sub-systems of a hypervelocity ballistic range, because it is the place where the test model/projectile flies and impacts the target. Observation windows are set up in the test section, for recording the projectile trajectory and the resulting flow field.

Most of the test models/projectiles fly freely inside the test section; however they could fly on a track in Range G at AEDC. To reach a pre-set flight ambient condition, the blast tank and test section all have their affiliate vacuum system, to control the pressure, temperature and component of the gas in the blast tank and in the test section. In hypervelocity impact tests, usually only vacuum condition should be simulated. However, to meet the need of other tests such as hypersonic aerodynamics and erosion/ablation of thermal protection materials, some special equipment has to be installed in the test section, including rain/snow field simulator, test model recovery system, etc.

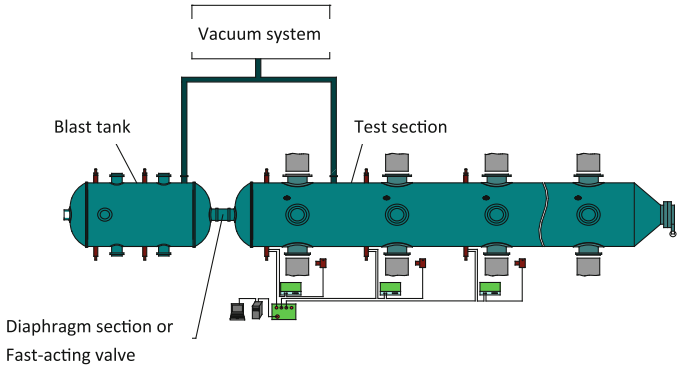

Fig. 5 Schematic of test chamber (gun shoots from *left* to *right*)

2.3 Measurement and Control System

The parameters to be measured are velocity of the tested model or projectile, its flight attitude, flow field structure, optical emission from the flow and from the tested model, surface pressure and heat flux on the tested model, shock wave parameters (such as pressure, temperature and shock wave speed in target material), velocity and geometry of the debris cloud, etc. The control system is to control different subsystems (such as gun, shadowgraphers, pulse light source, flash X-ray, etc.) of a ballistic range in order to ensure its working in a desired sequence. Because the flight speed of the tested model or projectile in a hypervelocity ballistic range is always as high as several kilometers per second, the time duration of model passing through a test station window is usually on the order of 10–100 μs. So it is not easy to accomplish all those measurement and control in a hypervelocity ballistic range test.

First of all, we have to detect the model or projectile which is flying at several kilometers per second at each measurement station. Non-contact methods could be adopted, such as radar, magnetic induction, optical emission detector. Photoelectric detection is the most common approach. A sheet of laser comes out from one side of the range chamber, perpendicular to the axis of the ballistic range. When the model or projectile flies through the laser sheet, either light decrease or light increase could be recorded by sensors on the other side of the range chamber. In this way, it is possible to know the exact time when the model or projectile arrives at the measuring station. Having at least two stations equipped with this kind of laser sheet, the velocity of the model or projectile could be easily calculated.

The second primary job of the measurement system is to visualize the flight attitude and the flow field around the model or projectile. High speed shadowgraph or flash X-ray is used, which cause no disturbance to the model's flight or to the evolved flow field. Along the test chamber of a ballistic range, there are always many test stations. The numbers of stations are different depending on the purpose

of the range. For an aero ballistic range, there might be as many as 50 test stations like in the AEDC Range G [12]. However, for an impact range, there are fewer test stations, because there is no need to record the model attitude variation along its flight path. At each station, usually a pair of orthogonal shadowgraph or schlieren or flash X-ray are installed to capture the attitude of the flight model or check the integrity of projectile before it impacts the target.

One of the important works at hypervelocity ballistic range is to measure the shock wave parameters in the target material which is generated by the projectile hypervelocity impact. The basic shock wave parameters are shock wave velocity and pressure, which can be obtained by using pressure sensors. Before a test, pressure sensors are placed at interesting points on the target surface or inside the target. During the test, a pressure history can be recorded by each of the used pressure sensors, thus the shock velocity can be obtained by comparing data obtained from at least two sensors. There are two types of pressure sensors, piezoresistive sensors and piezoelectric sensors. Polyvinylidene Fluoride (PVDF) is a piezoelectric sensor widely used in shock measurement. The other shock wave parameters, such as surface displacement and surface velocity can be obtained by using Velocity Interferometer System for Any Reflector (VISAR).

3 Representative Hypervelocity Ranges in the World

Since the 1950s, more than fifty hypervelocity ballistic ranges of different sizes have been built around the world. All of them have done good job in their research fields. However due to limited space, only a few most active ranges are introduced here. They are:

- AEDC Range G,
- Hypervelocity Free-Flight Aerodynamic Facility (HFFAF) of NASA Ames,
- hypervelocity ballistic ranges of the UAH Aerophysics Research Center (UAH-ARC),
- Hypervelocity Impact Test Facilities (HITF) of NASA JSC,
- Hypervelocity impact ranges of Ernst-Mach Institute (EMI),
- Hypervelocity Ballistic Range Complex of CARDC.

3.1 AEDC Range G

As the world's largest hypervelocity ballistic range, Range G was built in 1962 at the Arnold Engineering Development Centre of US Air Force [13]. A schematic diagram of Range G is shown in Fig. 6 [11]. Continued upgrades were carried out, for example a thorough upgrade of launchers and measurement systems in the 1990s, and upgrade of the data processing system in the year 2006.

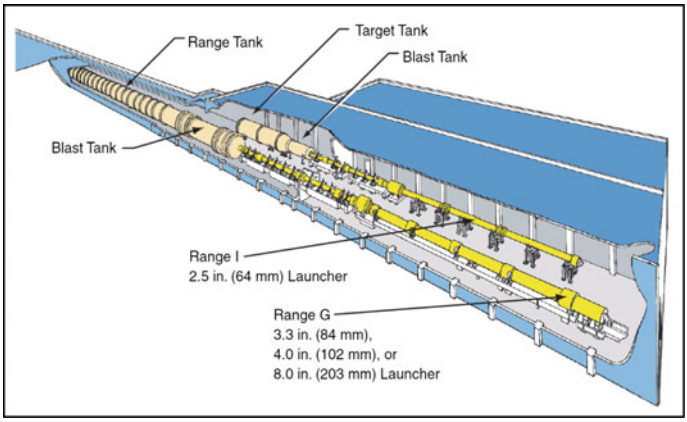

Fig. 6 Schematic of range G and range I [11]

Fig. 7 Launcher room of range G and range I [13]

Shown in Fig. 7 is the launcher room of Range G and Range I (which is a smaller range specifically for hypervelocity impact tests) [13]. The two-stage LGGs of Range G have launch tubes of 84, 102 and 203 mm bore diameters, respectively. The highest muzzle velocity is about 7 km/s, while the 203 mm gun can accelerate a 12 kg model to 4 km/s [14], and the 84 mm gun can accelerate a 908 g model to 6 km/s [15]. The launcher capability of Range G is shown in Fig. 4 [11]. The so-called "counter-fire" technique was developed by using two two-stage LLGs shooting face to face, achieving hypervelocity impact velocities greater than 12 km/s [16].

The test chamber, which is 3 m in diameter and about 300 m in length, it contains a unique track guidance system which is comprised of a four-rail system for model guidance and a 213.4 m-long model recovery system [14]. Besides of simulating the flight altitude by a vacuum system, the climatic cloud particles such as rain drops or ice crystal could be simulated in this test chamber [17].

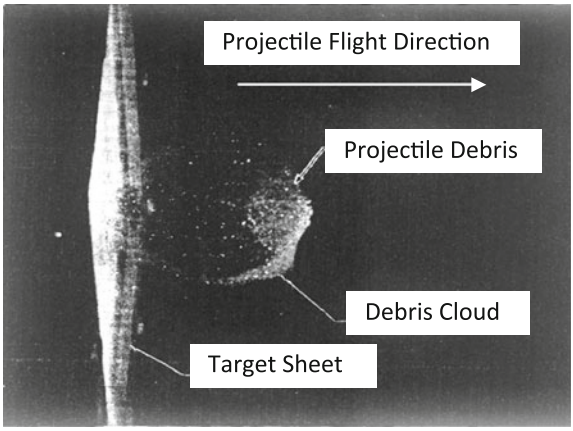

Fig. 8 Target sheet and debris cloud captured by front light imaging [15]

Powerful transient measurement instruments used in this facility, includes shadowgraph/schlieren, orthogonal flash X-ray, high-speed X-ray imaging system, ultra-high speed camera, laser front-light imager, multispectral/infrared signal measurement system, etc. [17].

Applications of Range G include tests of aerodynamics, erosion/ablation of Thermal Protection System (TPS) materials, boundary layer transition, rocket plume, re-entry aerophysics, hypervelocity impact, etc. For example, debris cloud in a hypervelocity impact test is shown in Fig. 8 [15].

3.2 HFFAF at NASA Ames Center

There are two hypervelocity ballistic ranges at NASA Ames research center. One is Ames vertical gun range (AVGR) built in 1964, which was designed to conduct experiments on lunar impact processes in support of the Apollo mission. The other is Hypervelocity Free-Flight Aerodynamic Facility (HFFAF) built in 1965, which is basically a multi-purpose range.

The HFFAF is a combined ballistic range and shock tunnel [18, 19], sketch of the facility is shown in Fig. 9. The HFFAF consists of: a model launcher (light-gas gun or powder gun), a sabot separation tank, a test section and impact/test chamber, a nozzle and a shock tube. There are four light-gas guns with launch tube bore diameters of 7.6, 12.7, 25.4, and 38.1 mm, and three powder guns with launch tube bore diameters of 20, 44, 61 mm, respectively. The highest muzzle velocity is 8.5 km/s. The test section is 22.86 m long with sixteen orthogonal shadowgraph stations as shown in Fig. 10. For very high Mach number (i.e. $M > 25$) simulation, models can be launched into a counter flowing gas stream generated by the shock tunnel [18].

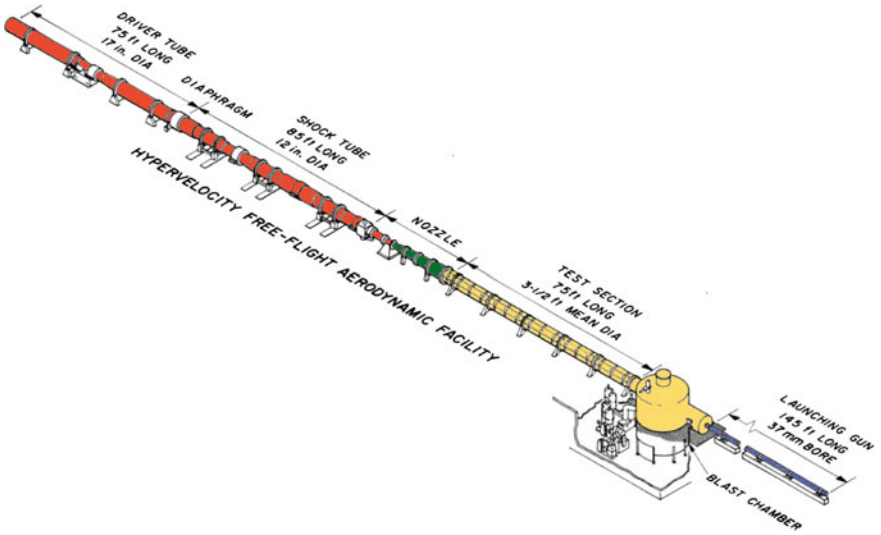

Fig. 9 Sketch of HFFAF at NASA Ames [19]

Fig. 10 HFFAF test section with sixteen shadowgraph stations [19]

The following studies have been carried out at HFFAF: earth atmospheric entry, planetary entry and vehicles aerobraking, scramjet propulsion, meteoroid/orbital debris, and various configurations for supersonic and hypersonic aircraft. The test models shot at HFFAF are shown in Fig. 11. As an example, Figs. 12 and 13 show a boundary layer transition experiment conducted at HFFAF.

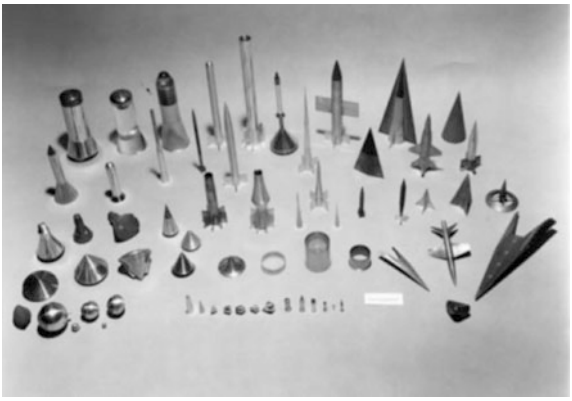

Fig. 11 Test models at HFFAF [20]

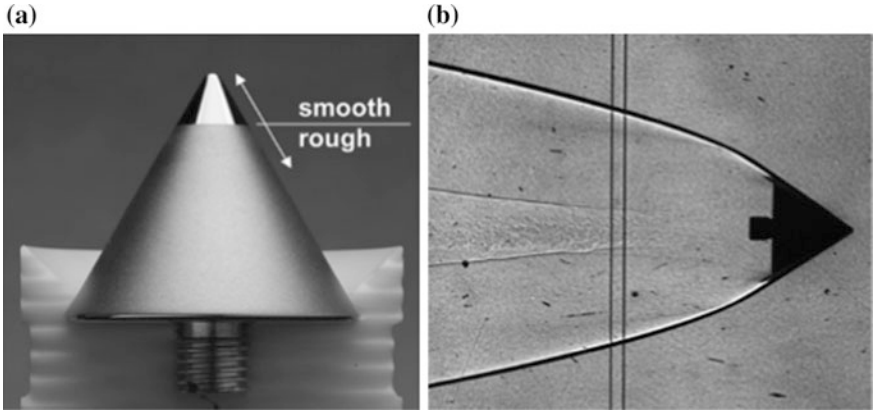

Fig. 12 Small-bluntness model, **a** mounted in launch sabot with half of sabot fingers removed, and **b** model in flight at $M_\infty = 10$ [20]

3.3 Hypervelocity Ballistic Ranges at ARC-UAH [21–23]

The three hypervelocity ballistic ranges of the University of Alabama in Huntsville, the Aerophysics Research Center (UAH-ARC) belonged to the Defense Laboratory of General Motors Corporation before the 1980s. Before and after the ranges were moved to UAH-ARC in Huntsville in the 1980s, and lots of hypervelocity impact and aerophysics experiments were conducted at the range. Though the ranges are run by UAH-ARC, their properties are owned by US Army.

There are a series of two-stage light gas guns at UAH-ARC, including a large range, an intermediate range and a small range, with launch bore diameters from 19 mm up to 152 mm. The maximum muzzle velocity is 8 km/s. The test chamber

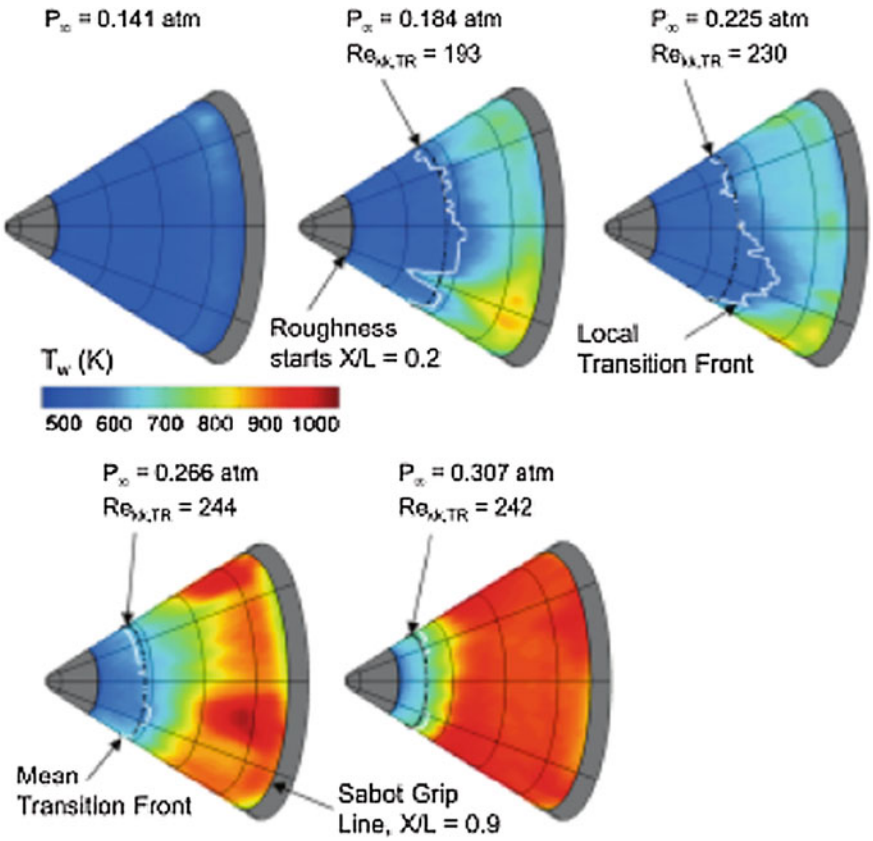

Fig. 13 Measured surface temperature distributions for the small-bluntness cones (obtained by several high speed thermal-imaging cameras) [20]

of the range for aerophysics tests is 3 m in diameter and 279 m long. Figure 14 shows the 152 mm two-stage LGG with 254 mm bore diameter pump tube and its launch capability.

The ranges are equipped with a full range of measurement instruments, such as flash X-ray imaging system, front light laser imaging system, shadowgraph/schlieren, CW Doppler radars (3, 9,17, 35, and 70 GHz), interferometers, radiometers (1.5–2 μm, 2–3 μm, 3–4 μm, 4–5.5 μm, 8–12 μm), spectrographer and others. Besides hypervelocity impact lethality tests, lots of aerophysics research could be carried out, such as wake structure, radar scattering characteristic, electron density distribution, optical radiation intensity and spectral properties. Figure 15 shows results from two of conducted tests.

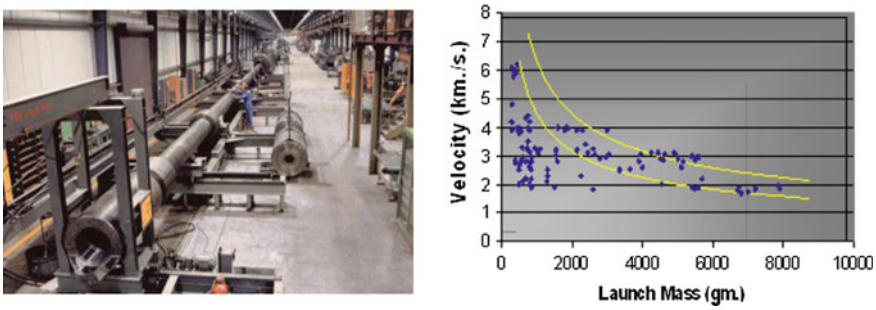

Fig. 14 The 152 mm two-stage LGG with 254 mm bore diameter pump tube and its launch capability [22]

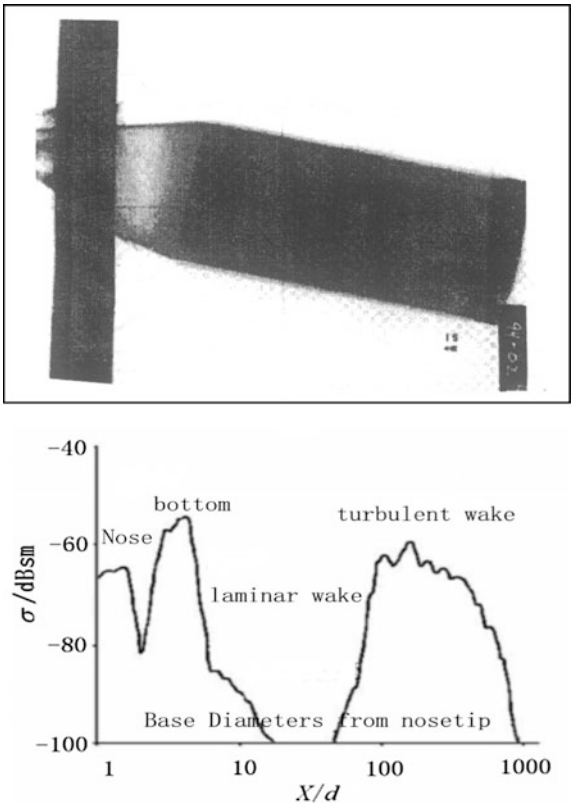

Fig. 15 Tests at UAH-ARC. *Upper* X-ray of a model impacting target. *Lower* radar cross section (RCS) of a hypervelocity vehicle and its wake [23]

3.4 Hypervelocity Impact Ranges at NASA JSC [24]

As the focus point in the development of protection shields for spacecrafts in the US, NASA Johnson Space Center (JSC) possesses a long history in hypervelocity impact tests of meteoroids and space debris. Now, there are four hypervelocity impact ranges at Hypervelocity Impact Test Facilities (HITF) of NASA JSC [24], one of which is shown in Fig. 16. The launch tube bore diameters of the two-stage LGGs are 25.4, 12.7, 4.3 and 0.18 mm, respectively. The measurement instruments consist of: laser detectors (shown in Fig. 17), high speed camera (shown in Fig. 18) and a flash X-ray (shown in Fig. 19). The high speed camera can obtain 80 images in one test at 2,500,000 frames/s.

Since the 1960s, many hypervelocity tests on spacecraft shield have been carried out at NASA JSC, trying to protect the Apollo command module, the space shuttle orbiter, the Hubble space telescope, the space suit like EMU, and the International Space Station (ISS). Based on traditional Whipple shield (A shield to protect spacecraft from meteoroid proposed by Fred Whipple in the 1940s), new shield

Fig. 16 Hypervelocity impact range at NASA-JSC

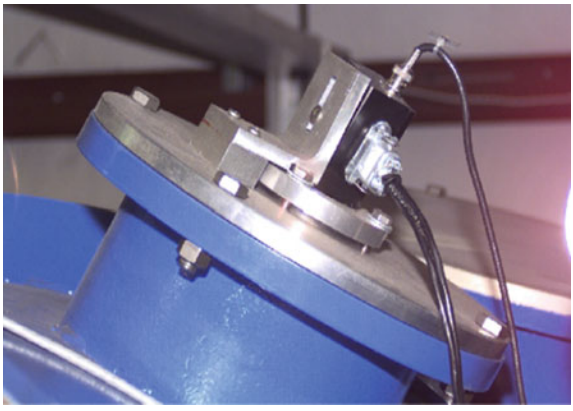

Fig. 17 Laser detectors

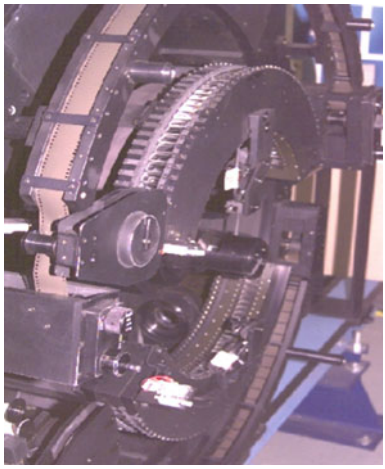

Fig. 18 High speed camera

Fig. 19 Flash X-ray heads

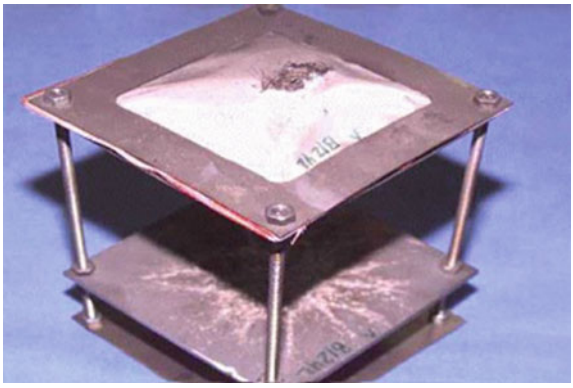

Fig. 20 β-cloth shield

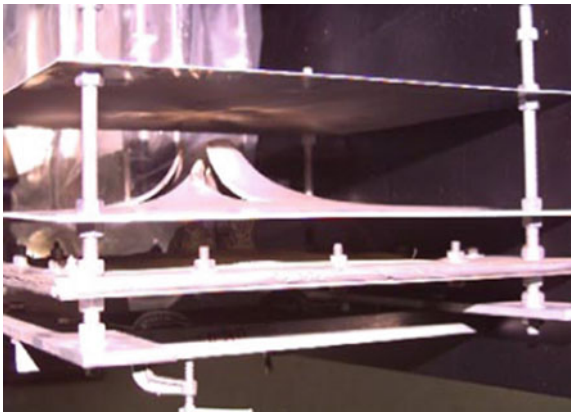

Fig. 21 Stuffed whipple shield

configurations have been developed by scientists and engineers at JSC, such as stuffed Whipple shield (Fig. 20), multi-shock shield, mesh double-bumper shield, and β-cloth shield (Fig. 21), etc.

3.5 Hypervelocity Impact Ranges at EMI, Germany

Currently, the Ernst Mach Institute (EMI) might be the most active institution in the field of hypervelocity impact in Europe. At EMI, three hypervelocity impact ranges (so-called small, medium, and large range) of different size are used for terminal ballistics, simulation of space debris and micrometeoroid impacts on spacecraft components, dynamic load on material with extra high pressure. Two of the ranges are shown in Fig. 22 [25].

The three ranges have similar configurations, including two-stage LGG, blast tank, sabot separation system, impact chamber and transient measurement instruments. The launch tube bore diameters range from 4 to 65 mm, and the highest muzzle velocity is 10 km/s with a 0.005 g projectile (Fig. 23) [25]. Projectiles as small as 100–500 μm could be launched by small light gas gun in shotgun mode

Fig. 22 Ballistic ranges at EMI (*Left* small, *right* medium) [25]

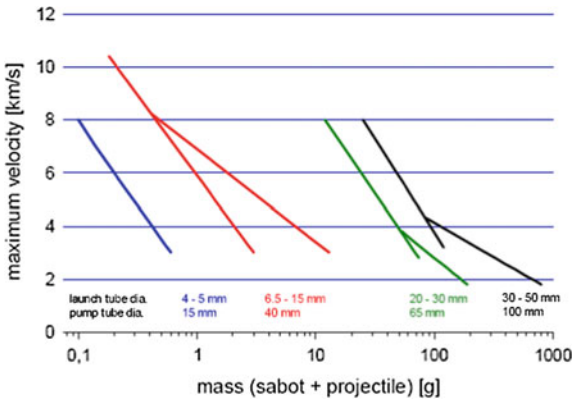

Fig. 23 Performance of EMI's light-gas guns [25]

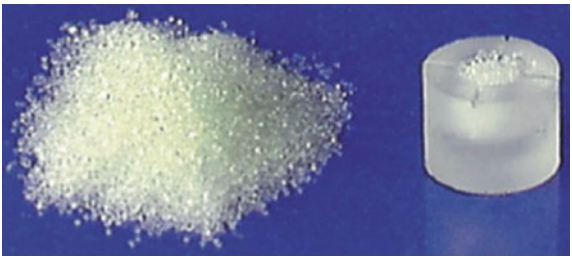

Fig. 24 Sabot (*right*) for projectiles (*left*) with diameter less than a millimeter [26]

(Fig. 24) [26]. The measurement system includes laser detectors, shadowgraph, flash X-ray, microwave radar velocimeter, high speed camera, image convertor camera, and ballistic pendulum [27].

Using the three ballistic ranges, EMI conducted large amounts of hypervelocity impact tests in the field of space debris and planetary physics. The related research works includes spacecraft shielding [28], vulnerability of satellite equipment under hypervelocity impact [29], Structural vibrations induced by hypervelocity impact [30]. planetary impact [31], Electrical signatures of hypervelocity impact plasma [32].

3.6 Hypervelocity Ballistic Range Complex of CARDC, China

At the largest hypervelocity ballistic range complex in China, there are four ranges at the Hypervelocity Aerodynamics Institute (HAI) of China Aerodynamics R. & D. Center (CARDC). The ranges were originally developed for studying hypervelocity

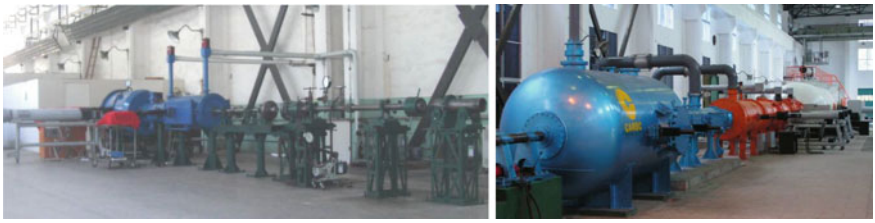

Fig. 25 Hypervelocity impact range A (*left*) and aerophysics range (*right*) of CARDC [33]

aerodynamics during the 70s of the previous century. As a result of space debris issue hypervelocity impact tests gradually became one of their primary works. For example, all the hypervelocity impact tests conducted for the first Chinese space lab "Tiangong-1" have been accomplished at this range complex.

The four ranges are Impact Range A (with 7.6 mm LGG,), Impact Range C (with 16 mm LGG), Aerophysics Range (with 25 mm LGG,), and 200 m Free Flight Range (37 and 50 mm LGG, shown in Fig. 2). Shown in Fig. 25 are Impact Range A and Aerophysics Range [33]. The highest muzzle velocity is 8.6 km/s at Impact Range C with a 180 mg projectile. The launch capability could be found in Fig. 4. While the impact chamber of Impact Range A is just 1 m in diameter and 1.8 m in length, the test chamber of the 200 m Free Flight Range is 1.5 m in diameter and 200 m in length, in which flight altitude and rain/snow could be simulated.

Transient measurement instruments at these ranges include laser detector, shadowgraph/schlieren, binoculars imaging system, high speed (5 million f/s) camera, eight-sequence laser shadowgraph, flash X-ray, visible and IR radiometer and spectograph, microwave interferometer, X and Ka band CW Doppler radar, etc.

The hypervelocity ballistic ranges at CARDC are applied for the studying hypervelocity aerodynamics/aerothermodynamics, rain/snow erosion of Thermal

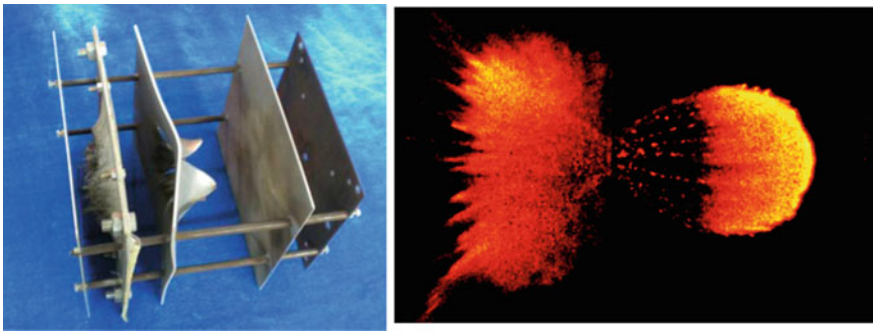

Fig. 26 Hypervelocity impact tests at CARDC. *Left* stuffed whipple shield. *Right* infrared image of debris cloud

Protection System (TPS) materials, hypervelocity impacts for spacecraft shields against space debris, aerophysics, etc. Shown in Fig. 26 are results from hypervelocity impact tests.

4 Application of a Hypervelocity Ballistic Range

A hypervelocity ballistic range is used to investigate phenomena pertinent to a hypervelocity flight body, to either reentry aerothermodynamics or Whipple shield against space debris. In general, the application of hypervelocity ballistic range falls into three categories, namely hypervelocity aerodynamics, hypervelocity aerophysics, and hypervelocity impact.

4.1 Hypervelocity Aerodynamics

Dynamic aerodynamic coefficient As for the study of hypervelocity aerodynamics, ballistic range is used to measure dynamic aerodynamic coefficients. When a model flies down the range, its time-of-flight is recorded by laser detectors. its flight speed is easily deduced from recorded passage time between two measuring stations whose separation distance is known. Optic apparatus, such as shadowgraph or schlieren and high speed camera enables recording the model time of arrival, its position, attitude, and also the flow field structure. Based on such information, the model trajectory and variations in its angle-of-attack along its trajectory could be re-constructed. Data reduction is applied to the trajectory and angle-of-attack data to determine dynamic aerodynamic coefficients, which determines the damping property of a re-entry vehicle. As for a blunted 5° half-angle cone flying at 5 km/s and at a Reynolds number of 10^6, the estimated error in measured coefficients is less than 3 %, as shown in Fig. 27.

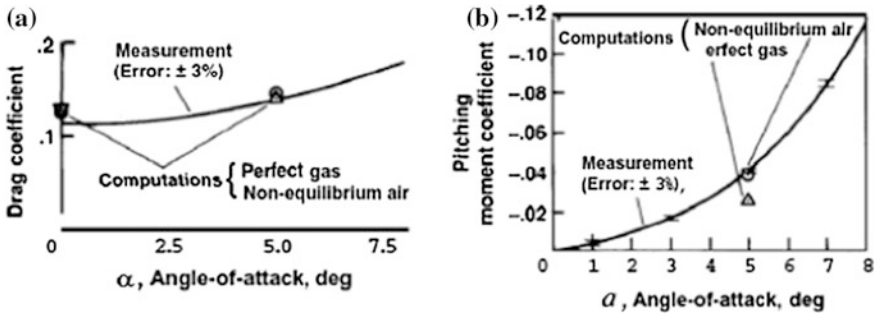

Fig. 27 Drag and pitching moment coefficient versus AOA of 1 blunt 5° half-angle cone [7]

Boundary layer transition One of the attributes of a ballistic range is the basically "quiet" flight condition compared with hypersonic wind tunnels and shock tunnels. Since the fluctuation and noise of the incoming flow at the nozzle exit may significantly affect the results of boundary layer transition at test model, the stationary, un-perturbed, un-contaminated test atmosphere inside the test section makes ballistic range a unique ground test facility in the regime of boundary layer transition research.

During the 60s and the 70s of the past century, Advisory Group for Aerospace Research and Development (AGARD) carried out tests on boundary layer transition both on the surface of a flight vehicle model and in its wake in ballistic range. Shown in Fig. 28 is a shadowgraph of turbulent boundary layer on a slender body of revolution at M = 3.5 and Re = 12×10^6 [4]. In Fig. 29, the turbulence burst is clearly shown [4]. Recently, under the hypersonic project of NASA's Fundamental Aeronautics Program, NASA Ames Centre carried out series of hypersonic boundary layer transition experiments at HFFAF, by using Intensified Charge

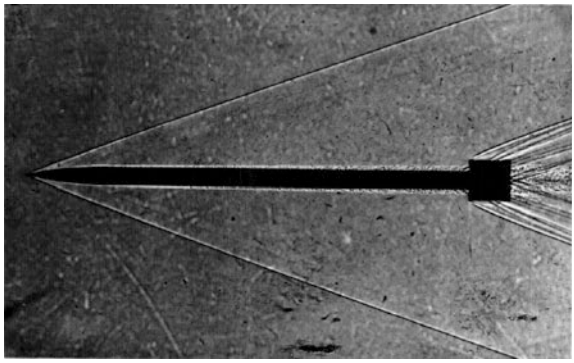

Fig. 28 Shadowgraph of turbulent boundary layer on a slender body of revolution at M = 3.5 and Re = 12×10^6 [4]

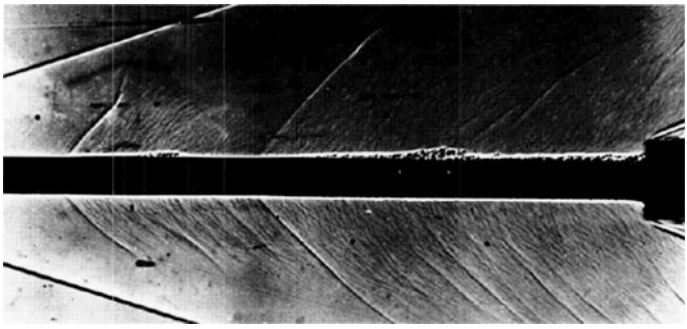

Fig. 29 Shadowgraph of isolated turbulence burst on a slender body of revolution at M = 3.5 [4]

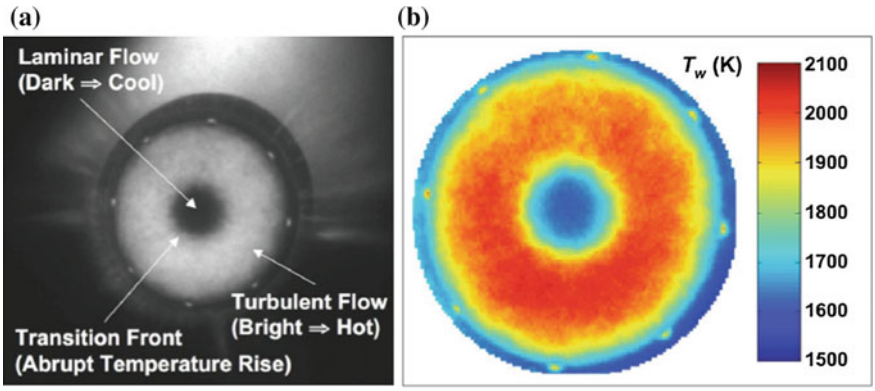

Fig. 30 Pre-ablated hemispherical POCO (graphite division of pure oil company) graphite nosetip Rn = 19.05 mm, V = 4.5 km/s, P = 0.317 atm; **a** ICCD camera image; **b** global surface temperature distribution [34]

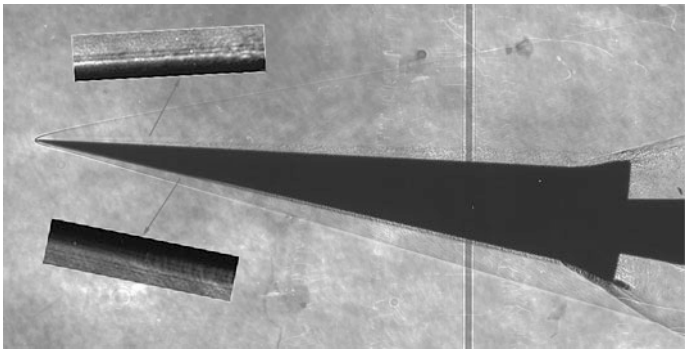

Fig. 31 Boundary layer transition test of slender cone M = 5.77, Re/L = 8.56×10^7, Re = 9.42×10^6, $\alpha = 7.9°$

Coupled Device (ICCD) to measure the transient temperature distribution on model surface. Shown in Fig. 30 is an infra-red image and reconstructed temperature distribution on a semi-spherical model [34, 35].

Shown in Fig. 31 are images of boundary layer transition experiment of a 5° sharp cone recently conducted at ballistic range of CARDC.

4.2 Hypervelocity Aerophysics

Aerophysics considers the interaction between hypervelocity moving objects and ambient gas environment into which it propagates. Due to the high temperature

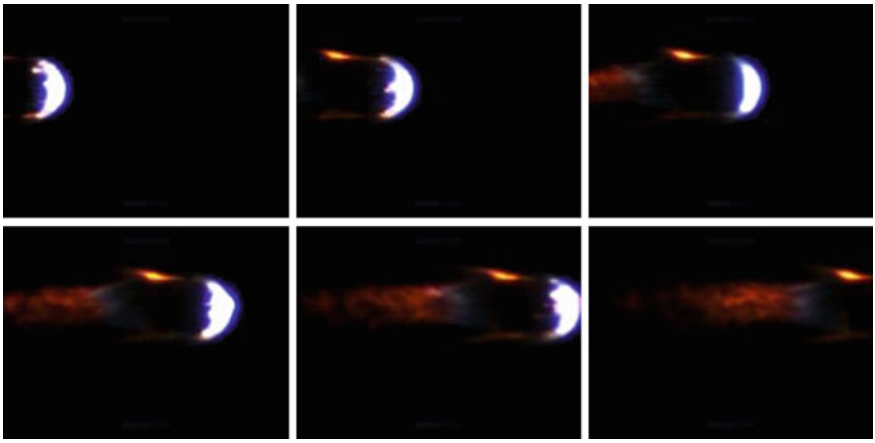

Fig. 32 Optical image of a flow field around hemispherical model at 5.0 km/s (from *upper left* to *lower right*, 186,000 fps, 1 μs exposure time)

generated around the travelling body real gas effects such as vibration, dissociation, electronic excitation, ionization, radiation and electromagnetic transmission and scattering must be considered.

Clean and un-contaminated flight environment makes hypervelocity ballistic range a unique ground test facility to reproduce phenomena associated with chemical reaction and electromagnetics. Main application of hypervelocity ballistic range in aerophysics include: measurement of optical emission, electron density in the plasma wake, electromagnetic scattering from the vehicle model and its wake. Shown in Fig. 32 is an image of a hypervelocity hemi-sphere model at the Hypervelocity Aerophisics Range of HAI at CARDC, showing the high temperature gas cap and the wake behind the hemi-sphere.

ARC-UAH and its predecessor, Delco System Operation of General Motor, have the most powerful hypervelocity ballistic range test capability in aerophysics phenomena. Typical instruments are visible to Long Wavelength Infrared (LWIR) optical emission radiometers, microwave interferometers and forward scattering radar for wake electron density measurement, and mono- and bi-static radar for Radar Cross-Section (RCS) and wake velocity measurement. Shown in Fig. 33 is RCS spectral energy of hypersonic sphere model wake obtained at ARC-UAH [21]. The curve shows the spectral function for wakes of spherical bodies. Shown in Fig. 34 is infra-red spectral radiation intensity of hypersonic wake obtained at Range G of AEDC [36]. The X axis in Fig. 34 is scaled in terms of distance behind the model nose in body diameters. A, B and C is referred to measurement locations at 130, 249 and 409 ft from range entrance, respectively.

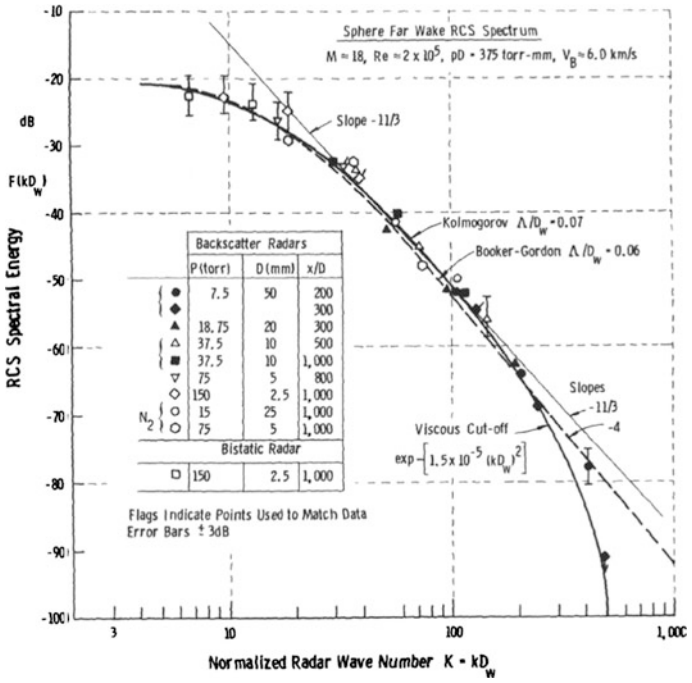

Fig. 33 RCS spectral energy of hypersonic sphere model wake obtained at ARC-UAH [21]

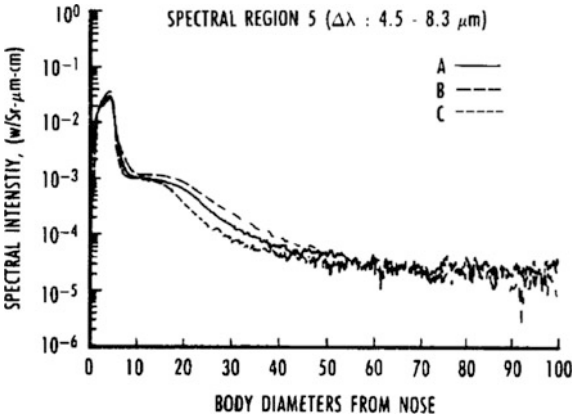

Fig. 34 Infra-red spectral radiation intensity of hypersonic model and wake [36]

4.3 Hypervelocity Impact

Studies of hypervelocity phenomena were motivated by issues such as meteor craters on the moon and other planets, interception of ballistic missiles, space debris protection of spacecraft, and solid state physics of materials at extremely high

pressures. The hypervelocity ballistic range (or may called as hypervelocity impact range in the considered case) is characterized by the formation of very strong shock waves in a hitted target, which results in very high pressure, measured in millions of atmospheres.

While the hypervelocity launcher and part of the instrumentation of the ballistic range used for impact studies are the same as those for aerodynamic tests, other subsystems might be essentially different and specialized. In hypervelocity impact tests, the instrumentation will be grouped around the target, including ultra high-speed cameras to record the externally visible impact processes, luminosity detectors, high speed flash X-ray to record the internal damage of target, and other electro-magnetic detectors. Special screens placed to catch and record the distribution of debris material ejected either forward or backward from the impact point may be installed in the impact chamber. And usually, the impacted target might be recovered and examined.

Hypervelocity impact experiments in ballistic range include the basic phenomenology of cratering, space debris impact on space structures, and the properties of materials at very high pressure [4].

Phenomenology of cratering Cratering is one of the most common phenomena in the development of planets, as seen on the moon and other planets. In planets case, the target is regarded as semi-infinite, that means its width and thickness are both many times greater than the size of the projectile, and that the reflected of shock wave from the target boundary has negligible effect on the penetration process of penetration. The most symbolic phenomenon of hypervelocity impact on a semi-infinite target is the semi-spherical crater. Target materials include metals, minerals, plastics, and organic substances. A typical eject debris, crater and SEM graph of hypervelocity impact are show in Fig. 35.

Space debris impact on space structures Numerous space debris of different sizes are now circling around the earth, and right now there is no reliable approach to clean this debris. One of the choices is to enhance the protection of our spacecraft against space debris. Many kinds of shields have been developed, based upon the concept of Whipple shield. All these newly developed shields have to be tested at hypervelocity impact ranges. Considering the damage evaluation of a spacecraft under hypervelocity impact, test articles could be more complicated, including

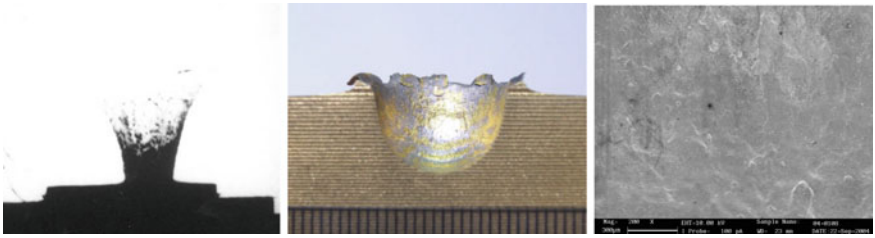

Fig. 35 Typical eject debris, crater and SEM graph under hypervelocity impact (∅3 mm copper ball impact copper semi-infinite target at 6.31 km/s, CARDC)

electronic box, fuel tank, solar cells, heat shields, propulsion units, space-suit, and even a real satellite. Reference [37] describe results of some of the many experiments in this field. A typical Whipple shield and shadowgraph of impact debris are shown in Fig. 36 [38].

Materials at very high pressure A third area of research is the study of material at high pressures attained behind the shock wave produced by impact of a high velocity projectile. The density and pressure in the shock-compressed zone can be determined by the velocity of shock propagation and of the material particle behind the shock front. The experimentally determined relation between these two quantities is generally termed the "Hugoniot" of the material, after the Rankine-Hugoniot relations describing the conditions across a shock wave (see Fig. 37). The material equation of state can be determined based on the Hugoniot findings,

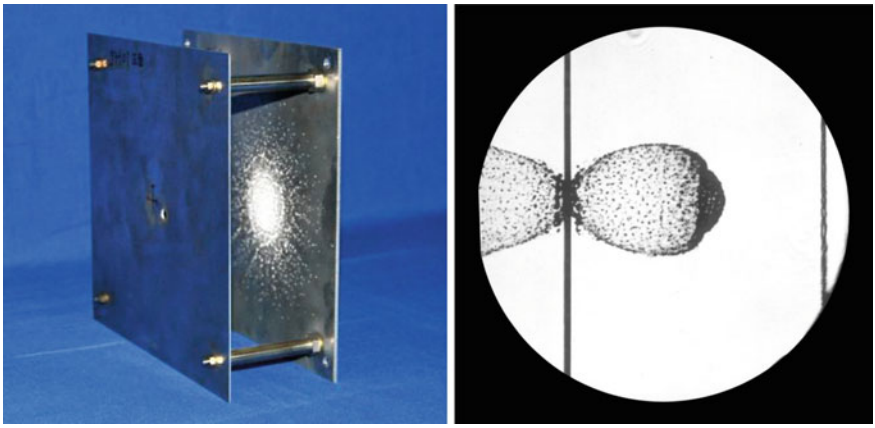

Fig. 36 Whipple shield and shadowgraph of debris cloud [38] (∅5.02 mm AL sphere impacts Whipple Shield at 5.52 km/s, CARDC)

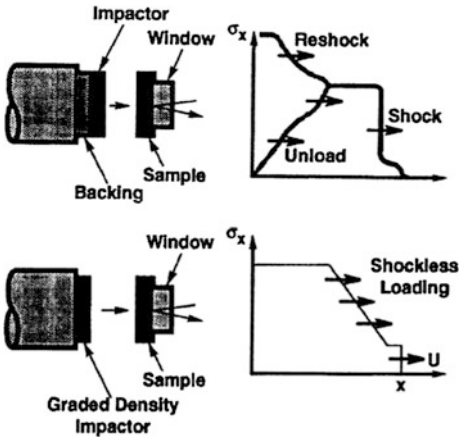

Fig. 37 Experimental techniques for off-Hugoniot measurements using gun-launched projectiles [41]

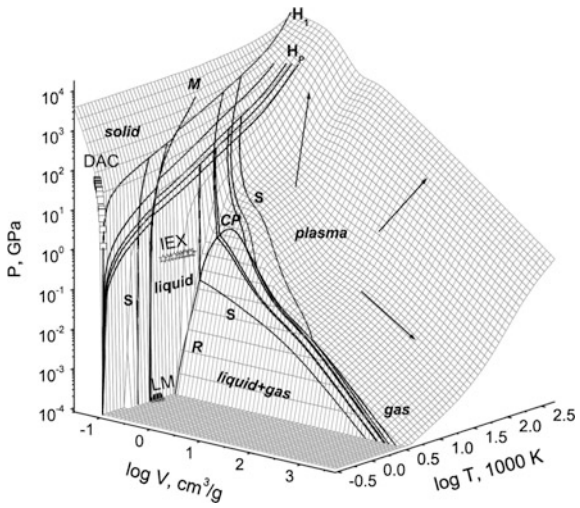

Fig. 38 3D surface of pressure-specific volume-temperature in copper [42]

(see Fig. 38). This is of great value in all scientific studies of solids at very high pressure (as e.g., studies of planetary interiors). An excellent description of this subject is given in Refs. [39, 40] including both analytical and experimental treatments.

5 Concluding Remarks

Ballistic range, especially hypervelocity ballistic range, have played a key role in researching phenomena resulted from a hypervelocity moving body in/out of the earth atmosphere or upon its impact on another object. In both fields of hypervelocity aerodynamics/aerothermodynamics and dynamic response of material/structure under hypervelocity impact, ballistic range is a main investigation tool. So far, it is the only experimental approach besides the real flight test that could provide us reliable hypervelocity data.

The advantage of hypervelocity ballistic range is that it could reproduce real hypervelocity scenery. For example, when we are interested in hypervelocity aerodynamics, the nature of free flight and non-contaminated ambient test gas makes ballistic range a better means (compared with hypersonic wind tunnels or shock tunnels) in obtaining important data such as boundary layer transition, optical emission, etc.

However, the disadvantage of hypervelocity ballistic range is also obvious: first, the relatively small model size limited by launch tube bore of a two-stage LGG; second, the difficulty in obtaining accurate measurements of that fast flying small test model/projectile.

Encouragingly, efforts have been made or are being made to further improve the test capabilities of hypervelocity ballistic ranges, such as the upgrade of the launcher and the measurement system at AEDC Range G in the 1990s. Right now at Hypervelocity Aerodynamics Institute of CARDC, the 200 m Free Flight Range is under upgrading process. Two-stage LGGs of 120 and 203 mm launch tube bore diameters are under fabrication, and the original 1.5 m diameter test section has been replaced by a 3 m diameter test section.

With bigger launcher and soft launch capability, more complicated flight vehicle models than those of today could be fired at hypervelocity, giving us greater chance to obtain desired experimental data than ever before. Together with the fast development of optical-electro instruments, miniature sensors based on Nano technology, and telemetry technology, hypervelocity ballistic range could hopefully be developed into a both reliable and affordable bridge between lab tests and real flight tests at outdoor range.

Acknowledgments The author would like to express sincere appreciation to Mr. Jinyang LUO, Mr. Yi LI, Mrs. Jie HUANG, Mr. Anhua SHI, Dr. Zhefeng YU, Mr. Hong CHEN, Mr. Dezhi JIAO, Mr. Fawei KE, Mrs. Lei ZHENG, and Mr. Yijian YAN for their invaluable help in the completion of this chapter.

References

1. National historic mechanical engineering landmark-aerodynamic range, The American Society Of Mechanical Engineers (1982)
2. Crozier, W.D., Hume, W.: High-velocity light gas gun. J. Appl. Phys. **28**(8), 892–894 (1957)
3. Pope, A., Goin, KL.: High-Speed Wind Tunnel Testing. Wiley, New York (1965)
4. Canning, T.N., Seiff, A., James, C.: Ballistic range technology, AGARDograph No. 138 (1970)
5. Lukasiewicz, J.: Experimental Methods of Hypersonics. Marcel Dekker, Inc, New York (1973)
6. Reda, D.C.: Correlation of nosetip boundary layer transition data measures in ballistic-range experiments, AIAA 1980-0286
7. Strawa, A.W., Chapman, G.T., et al.: Ballistic range and aerothermodynamic testing. J. Aircr. **28**(7) (1991)
8. Chapman, G.T.: The ballistic range—Its role and future in aerothermodynamic testing, AIAA 1992-3996
9. Jiang, W.B., et al.: Design of hypersonic test facilities, Press House of Defense Industry (of China) (2001)
10. Lu, F., Marren, D.: Advanced hypersonic test facilities. AIAA series of Progress in Astronautics and Aeronautics, vol. 138 (2002)
11. Impact and lethality Testing[EB/OL]. http://www.arnold.af.mil
12. Cable, A.J.: Upgrade of the ballistic range facilities at AEDC: now complete. AIAA-94-2493
13. http://www.arnold.af.mil
14. Carver, D., Campbell, L.L., Roebuck, B.: Large-scale, hypervelocity, high-fidelity interceptor lethality development in AEDC's range G. Int. J. Impact Eng. 35–1459 (2008)
15. Campbell, L.L., Cable, A.J.: The upgraded ballistic range facilities at aedc. Int. J. Impact Eng. **17**, 131–138 (1995)

16. Young, R.P., Rushing, J.R.: Expanded impact test capabilities of the aronold engineering development center, AIAA 96-4241
17. Cable, A.J.: Upgrade of the ballistic range facilities at AEDC: the half-way point, AIAA-92–3997
18. Salinas, I.T., Cornelison, C.: Test planning guide for ASF facilities. 029-9701-XM3 Rev. B March (1999)
19. Grinstead, J.H., Wilder, M.C., Reda, DC., Cornelison, CJ.: Shock tube and ballistic range facilities at NASA ames research center. Technical report RTO-EN-AVT-186, NATO (2010)
20. Reda, D.C., Wilder, M.C.: Transition experiments on blunt cones with distributed roughness in hypersonic flight. J. Spacecraft Rockets **50**(3), 504–507 (2013)
21. Hayami, R.A.: The application of light gas gun facilities for hypervelocity aerophysics research, AIAA 92-3998
22. http://www.uah.edu/UAH/facilities.asp.htm
23. Liquornik, D.J., Yang, F.W., Zwiener, M.C., etc.: Active attitude control of gun launched projectiles. Int. J. Impact Eng. **23,** 561–572 (1999)
24. http://hitf.jsc.nasa.gov/NASAJSCLGG/nasajscgun/HITFHVITestingHighSpeedCameras.htm
25. Stilp, A.J.: Aeroballistic and impact physics research at emi and historical overview. Int. J. Impact Eng. **17**, 785–805 (1995)
26. Alwes, D.: Columnus-viewport glass plane hypervelocity impact testing and analysis. Int. J. Impact Eng. **10**, 1–22 (1990)
27. Destefanis, R., Faraud, M.: Testing of advanced materials for high resistance debris shielding. Int. J. Impact Eng. **20**, 209–222 (1997)
28. Thoma, K., Schäfer, F., Hiermaier, S., et al.: An approach to achieve progress in spacecraft shielding. Adv. Space Res. **34**, 1063–1075 (2004)
29. Schäfer, F., Putzar, R., Lambert, M., et al.: Vulnerability of satellite equipment to hypervelocity impacts. 59th International Astronautical Congress (2008)
30. Vergniaud, J.B., Guyot, M., Lambert, M., et al.: Structural vibrations induced by HVI—Application to the Gaïa spacecraft. Int. J. Impact Eng. **35**, 1836–1843 (2008)
31. Hoerth, T., Schafer, F., Thoma, K., et al.: Hypervelocity impacts on dry and wet sandstone: observations of ejecta dynamics and crater growth. Meteorit. Planet. Sci. **48**(1), 23–32 (2013)
32. Rudolph, M., Schimmerohn, M., Osterholz, J., et al.: Electrical signatures of hypervelocity impact plasma with applications in in-situ particle detection. Acta Astronaut. **101**, 157–164 (2014)
33. Liu, S., Huang, J., Li, Y.: Hypervelocity impact tests for spacecraft against orbital debris at HAI, CARDC. 59th International Astronautical Congress (2008)
34. Reda, D.C., et al.: Aerothermodynamic testing of ablative reentry vehicle nosetip materials in hypersonic ballistic-range environments, AIAA 2004-6829
35. Wilder, M.C., et al. Free-flight measurements of convective heat transfer rates in hypersonic ballistic-range environments, AIAA 2007-4404
36. Harris, H., Hendix, R.: Upgrade in optical measurement capabilities of AEDC ballistic ranges, AIAA 1994-0672
37. IADC WG3 members. Protection manual. IADC-WD-00-03 Version 4.0, Revision 8. March 12 (2010)
38. Liu, S., Li, Y., Huang, J., Luo, JY., Xie, A.M., Shi, A.H.: Hypervelocity impact test results of whipple shield for the validation of numerical simulation. J. Astronaut. **26**(4) (2005)
39. Mayer, M.A.: Dynamic Behavior of Materials. Wiley, New York (1994)
40. Solid State Physics, vol. 6, pp. 1–63. Academic Press. Inc., New York (1958)
41. Asay, J.R.: The use of shock-structure methods for evaluating high-pressure material propertics. Int. J. Impact Eng. **20**, 27–61 (1997)
42. Sultanov, V.G., Kim, V.V., Lomonosov, I.V., et al.: Numerical modeling of deep impact experiment. Int. J. Impact Eng **35**, 1816–1820 (2008)

Author Biography

Sen Liu is well-known for his studies in hypervelocity Impact and hypersonic aerodynamics at China Aerodynamics Research and Development Center (CARDC). He has worked as the head of Hypervelocity Ballistic Range Laboratory, Chief Scientist of Hypervelocity Aerodynamics Institute of CARDC. He is the vice-chairman of both the Committee of Hypersonic Aerodynamics and the Committee of Flow Visualization under the Chinese Society of Aerodynamics. Also, he is the associate editor-in-chief of the Journal of Experiments in Fluid Mechanics. He received his Bachelor and doctor degrees from Department of Aircraft at Northwestern Polytechnical University, and Master degree from the graduate school of CARDC. His current research mainly deals with hypervelocity impact of space debris against spacecraft, hypersonic boundary layer transition, and high temperature aerothermodynamics.

http://www.springer.com/978-3-319-26016-7

Hypervelocity Launchers

Seiler, F.; Igra, O. (Eds.)

2016, X, 300 p. 282 illus., 143 illus. in color., Hardcover
ISBN: 978-3-319-26016-7